

# Chinese Herbal Medicine Classification Based on BP Neural Network

Changjiang Liu<sup>a,c</sup>, Xuling Wu<sup>b</sup>, Wei Xiong<sup>c</sup>

<sup>a</sup> School of Science, Sichuan University of Science & Engineering, Zigong 643000, China  
Email: liuchangjiang@189.cn

<sup>b</sup> School of Foreign Language, Sichuan University of Science & Engineering, Zigong 643000, China  
Email: wx1519may@163.com

<sup>c</sup> School of Computer Science, Sichuan University, Chengdu 610065, China  
Email: xiongweib@scu.edu.cn

**Abstract**—A neural network model for classifying the Chinese herbal medicine based on image feature has been developed. The key process of the approach is to extract medicinal target region (region of interest, ROI). Two different auto-segmentation methods were adopted according to whether there were hollow in the medicinal materials. Subsequently, color, texture and shape feature of ROI was computed. Feature vector composed of forgoing features was input to back propagation neural network (BPN), with the class label as the output of neural network. BPN was trained mutually to classify the medicinal materials. The results of the experiment on 8 kinds of herbal medicine show the algorithms are valid with 98 high precision, with the structure of a 39-12-1 back propagation net.

**Index Terms**—Chinese herbal medicine (CHM), classification, back propagation neural network (BPN), region growing, image processing

## I. INTRODUCTION

**T**RADITIONAL Chinese medicine (TCM) has a history of thousands of years in China. Currently, due to its distinguished therapeutic effects with minimal or negligible side effects, TCM is gaining increasing attention around the world. However Chinese medicinal materials have a wide range of types from different areas, thus to discriminate alternatives and fakes by skilled pharmaceutical worker is labor-intensive and time-consuming. Furthermore the results of examination are vulnerable to influence by artificial factors. And it lacks efficiency and inheritance of experience. With the development of computerized image analysis, computer aided procession is applied in the identification and quantitative analysis of TCM.

In the research of TCM, analytic method mainly comprises bio-chromatographic methods[1], chromatographic methods[2-4], spectroscopic methods[5,6] and a combination of chemical and biological methods[7-10]. Fong et al.

introduced biopharmaceutical classification system (BCS) into the area of Chinese herbal medicine, and categorized CHM into four classes in terms of its solubility and permeability of active drug ingredient. Hou and Fang et al. used gas chromatography-pattern recognition to identify the TCM. Wang et al. developed the correlation analysis of the chemical fingerprint and biological effect, and assessed the quality of TCM. Computerized image analysis has been used in TCM identification. Wang et al.[9] presented a computerized facial image analysis system by using quantitative chromatic features for disease diagnosis applications. TCM feature extraction may be implemented from aforementioned methods, while it is not feasible to batch inspection industrially.

In this paper we propose the image feature (color, texture, shape feature) instead, only relying on image sensor with no reagent or other instruments. Firstly, TCM images are captured from image sensor. Secondly, target area of medicinal herbs is extracted. Then the color, texture, shape feature of the target region are formed to construct high dimension feature vector. In the end we select BPN as classifier to identify and grade CHM.

## II. OUTLINE OF CHM CLASSIFICATION PROPOSED

CHM classification based on BPN is made up of two major phases: training and classification procession. During the training period, after automatic detection of medicinal target regions (ROI), we extract the features of ROI to construct feature vector as input of BPN. The classification result from professionals is the desired net output. Finally, net is trained to get net parameters. The training procession is as shown in Fig.1. During the classification period, the feature is extracted by the same procession as in the training phase. Then the feature vector is input to the net with the attained net parameters from former phase, the simulation result is the final class label. The training procession is as shown in Fig.2.

## III. IMAGE FEATURES OF CHM

To extract proper image features is the most fundamental and important step, which decides the accuracy of classification. For the first step, alternative segmentations

Manuscript received July 26, 2013; revised September 5, 2013; accepted September 7, 2013.

This work was supported in part by the Foundation of Sichuan University of Science & Engineering (GrantNo.2012KY07), and the Science Foundation of Sichuan Province (GrantNo.2013FZ0032). This work was also supported by the high-quality goods resource sharing courses "mathematical modeling" of Sichuan province (GrantNo. 2012-57) and "mathematical modeling teaching group" of Sichuan University of Science & Engineering (GrantNo. 2009-142-01).

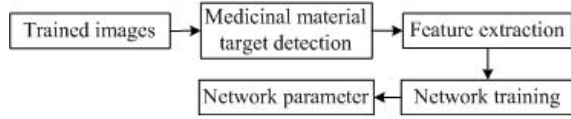


Figure 1. Network training procession

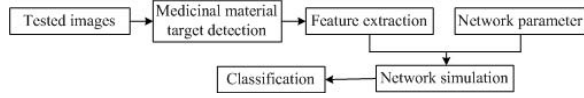


Figure 2. Network classification procession

are selected on the condition that the structure of herb medicine is hollow or not. And image features of medicinal target region are computed including color, texture and shape feature.

### A. Segmentation of medicinal region

Chinese medicinal materials are placed on the singular color background, and image acquisition is implemented in the photography box. In the course of acquisition, illumination keeps stable with high frequency and no blinking. Due to the uniform color of background, namely the region of non-medicine target can be flood filled via region growing algorithm. Thereby medicinal target regions are isolated from background.

The key to region growing algorithm is: (1) the choice of seed points; (2) the definition of threshold of growing. In this paper, the points on the four corners of image shown in Fig.3 are initial seed regions. They not only speed up convergence because of the abundant points, but also improve robustness for the directions of initial seed points.

Denote spotted regions in Fig.3 by  $R_0$ , and the region after  $n$  iterations of region-growing by  $R_n$ . Let  $f_k(i, j), k = 1, 2, 3$  be the red, green, blue component of the pixel at the  $i^{th}$  row  $j^{th}$  column of the image. In region growing, let the initial seeds have the gray value 255. If the points in the eight-neighborhood of the seed points satisfy similarity constraints, then are merged to the region assigning gray value 255. Simultaneously

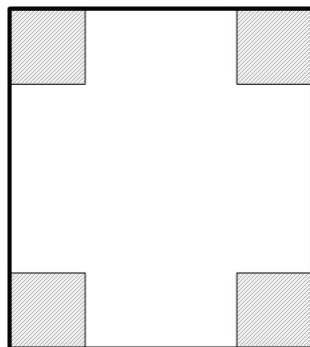


Figure 3. Initial seed regions (spotted)

the initial seeds and points merged become the next seed region. In succession, let last grown region be the seed region, region growing iterate until no points in eight-neighborhood satisfied the similarity constraints. The procession is described as Eq.1:

$$R_n = \{R_{n-1} \cup \{(i, j)\} | |f_k(i, j) - f_k(i_0, j_0)| \leq T_0, 0 \leq |i - i_0| \leq 1, 0 \leq |j - j_0| \leq 1, (i_0, j_0) \in R_{n-1}\} \quad (1)$$

After the background is filled, we denote the growing region by  $R$ . As a result of region growing algorithm, the medicinal image is segmented into medicinal target region and background region. The medicinal region is assigned to gray value 255 while the background region is assigned to 0 which is shown in Eq.2.

$$B(i, j) = \begin{cases} 255, & (i, j) \in R \\ 0, & else \end{cases} \quad (2)$$

Eventually the region which the image covers

$$I = \{(i, j) | 0 \leq i \leq W - 1, 0 \leq j \leq H - 1\}$$

is split up into

$$I = B_b \cup B_o, B_b \cap B_o = \emptyset \quad (3)$$

where

$$B_b = \{(i, j) \in B | B(i, j) = 0\},$$

$$B_o = \{(i, j) \in B | B(i, j) = 255\}.$$

Some images of herbal medicine, such as haw slice image, have hollow part. For this sort of herb, background region will be separated as well from medicinal region  $B_o$ . Apply contour tracing to binary image  $B$  and divide  $B_o$  into  $M$  disjoint connected components as follows:  $B_o = \bigcup_{k=1}^M B_o^{(k)}$ , where  $B_o^{(k)} \cap B_o^{(l)} = \emptyset, k \neq l$ .

Convert color of pixels in medicinal herb region  $B_o(k)$  into gray level according to Eq.4.

$$g_k(i, j) = 0.114f_1(i, j) + 0.587f_2(i, j) + 0.299f_3(i, j), (i, j) \in B_o^{(k)} \quad (4)$$

Ostu algorithm[11] is applied to threshold segment the image  $g_k$  adaptively. Denote the threshold of image  $g_k$  by  $T_k$ . Regard the points located on boundary  $\partial B_o^{(k)}$  as the representative elements of medicinal target region, calculate their average value  $\bar{g}_k$ . Judge whether the points in region  $B_o^{(k)}$  belong to the medicinal target region on the basis of the relationship between  $\bar{g}_k$  and threshold  $T_k$ . Specifically, if  $\bar{g}_k \geq T_k$ , the points whose gray value is greater than  $T_k$  in region  $B_o^{(k)}$  is considered as the points in medicinal target region and vice versa.

Associate with Eq.3, the medicinal target region is decided as below,

If  $\bar{g}_k \geq T_k$ ,

$$O_k(i, j) = \begin{cases} 0, & (i, j) \in B_b^{(k)} \\ 0, & (i, j) \in B_o^{(k)}, g_k(i, j) \leq T_k \\ 255, & (i, j) \in B_o^{(k)}, g_k(i, j) > T_k \end{cases} \quad (5)$$

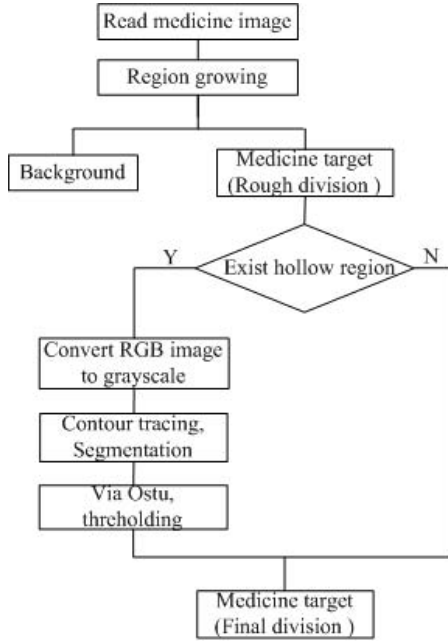


Figure 4. Flowchart of extraction of medicine target

If  $\bar{g}_k < T_k$ ,

$$O_k(i, j) = \begin{cases} 0, & (i, j) \in B_b^{(k)} \\ 0, & (i, j) \in B_o^{(k)}, g_k(i, j) \geq T_k \\ 255, & (i, j) \in B_o^{(k)}, g_k(i, j) < T_k \end{cases} \quad (6)$$

In the ultimate segmentation result, the region in which the points are assigned the gray value 255 is medicinal target region, a.k.a. ROI.

In detail, for medicinal herb with hollow part, after Eq.5 or Eq.6, ROI refers to Eq.7,

$$ROI = \{(i, j) \in I | O_k(i, j) = 255, k = 1, 2, \dots, M\} \quad (7)$$

For medicinal herb without hollow part, after Eq.2, ROI refers to Eq.8,

$$ROI = \{(i, j) \in I | B(i, j) = 0\} \quad (8)$$

**B. Features of medicinal herb image**

There are two principles to be followed as for selecting medicinal herb features: (1) for different kinds of herbs, huge difference exists in selected herb features; while for the same kind of herbs there exists little difference. (2) Consider the difficulty of network trained and the speed of network tested when combining and selecting the features. The feature selected is conducted in terms of the color, texture and shape.

1) *Color feature:* We mainly compute three parameters of color feature: average value, mean square deviation and entropy. Note the number of points in ROI as  $N$ , the number of pixels whose component gray value is  $l$  in ROI as  $n_l$ , and suppose the gray scale is  $L$ , then average  $u_k$ ,

mean square deviation  $\sigma_k$ , entropy  $e_k$  can be calculated as

$$u_k = \frac{1}{N} \sum_{(i,j) \in ROI} f_k(i, j) \quad (9)$$

$$\sigma_k = \sqrt{\frac{1}{N} \sum_{(i,j) \in ROI} (f_k(i, j) - u_k)^2} \quad (10)$$

$$p_l = \frac{n_l}{N}, l = 1, 2, \dots, L$$

$$e_k = - \sum_{l=1}^L p_l \log_2 p_l \quad (11)$$

The average value of images reflects the overall features of image color, which is one of the basic features of image. The average value of image is not connected with the spatial location of the gray value. It only reflects image brightness. Mean square deviation offers more abundant information than average value and is used to measure contrast of gray value. Entropy reflects the average amount of information in the image.

2) *Texture feature:* An important approach to region description is to quantize the texture. Texture is the characteristic of object surface. It shows the organizational structure of the surface and its sequence. This paper quantizes the texture by unifying local binary pattern LBP and gray level co-occurrence matrix.

Local binary pattern is a convincing texture description which is widely used in many areas of image processing such as face recognition and defect detection [12,13], etc. Suppose current pixel as center of neighbor, and compare gray value of the pixels around within a certain neighbor radius. Thus a group of binary number is worked out based on the quantity relation between the current pixel and center one. The local binary pattern LBP is

$$LBP_{P,R} = \sum_{p=0}^{P-1} s(g_p - g_c) 2^p$$

$$\text{Where } s(x) = \begin{cases} 1, & x \geq 0 \\ 0, & x < 0 \end{cases} \quad (12)$$

Here  $g(c)$  and  $g(p)$  refers to the pixels on the centre and boundary of the neighborhood respectively.

Aiming at solving the problem of too many binary patterns in traditional LBP, Ojala[14] put forward an unified binary pattern  $LBP_{P,R}^{riu2}$ :

$$LBP_{P,R}^{riu2} = \begin{cases} \sum_{p=0}^{P-1} s(g_p - g_c), & \text{if } u(LBP_{P,R}) \leq 2 \\ P + 1, & \text{else} \end{cases}$$

$$u(LBP_{P,R}) = |s(g_{p-1} - g_c) - s(g_0 - g_c)| +$$

$$\sum_{p=1}^{P-1} |s(g_p - g_c) - s(g_{p-1} - g_c)| \quad (13)$$

Gray level co-occurrence matrix[15](GLCM) is a common approach to describe texture by studying the related spatial features of gray level.

As a texture statistical method, gray level co-occurrence matrix is first put forward by Haralick in 1973. An arbitrary point  $(x, y)$  in the image and another point  $(x + a, y + b)$  constitute a point pair. If the gray value of these two points is  $i$  and  $j$  respectively, thus this point pair value is  $(i, j)$ . When taking different value of  $(a, b)$ , gray level co-occurrence matrix is obtained along a certain direction  $\theta$  and at a certain interval  $d = \sqrt{a^2 + b^2}$ . When the frequency of every  $(i, j)$  is calculated as  $\mathbf{P}(i, j, d, \theta)$ , the computed matrix of every  $(i, j)$  is gray level co-occurrence matrix. Here  $\theta$  usually take the value of  $0^\circ, 45^\circ, 90^\circ$  and  $135^\circ$ . Therefore, gray level co-occurrence matrix of these directions is computed. Then the angular second moment  $W_1$ , contrast  $W_2$ , relativity  $W_3$  and entropy  $W_4$  are worked out. The average of corresponding value in these directions is taken to be texture feature.

Angular second moment:

$$W_1 = \left( \sum_{k=0}^3 \sum_{i=1}^g \sum_{j=1}^g \mathbf{P}^2(i, j, d, k\frac{\pi}{4}) \right) / 4$$

Contrast:

$$W_2 = \sum_{i=1}^g \sum_{j=1}^g [(i - j)^2 \mathbf{P}(i, j, d, \theta)]$$

Relativity:

$$W_3 = \sum_{i=1}^g \sum_{j=1}^g \frac{ij \mathbf{P}(i, j, d, \theta) - u_1 u_2}{d_1 d_2}$$

In which

$$u_1 = \sum_{i=1}^g i \sum_{j=1}^g \mathbf{P}(i, j, d, \theta), u_2 = \sum_{i=1}^g j \sum_{j=1}^g \mathbf{P}(i, j, d, \theta)$$

$$d_1^2 = \sum_{i=1}^g (i - u_1)^2 \sum_{j=1}^g \mathbf{P}(i, j, d, \theta),$$

$$d_2^2 = \sum_{i=1}^g \sum_{j=1}^g (j - u_2)^2 \mathbf{P}(i, j, d, \theta)$$

3) *Shape feature*: The shape of an image is the most important visual feature in image features. The description of shape feature involves the description of contour boundary, namely perimeter and the region within the boundary, namely area. In medicine classification system, we introduce the width-height ratio and roundness of the minimum bounding rectangle to describe the shape feature.

Six Hu moments are also employed in medicine classification system.

The width and height of the bounding rectangle is  $w$  and  $h$  respectively. Suppose the width-height ratio is  $asp = \frac{w}{h}$ .

The roundness is defined as  $r = \frac{C^2}{A}$ , where  $C, A$  is perimeter and area of contouring region respectively.

In computing Hu moments, firstly convert the colored image into gray scale image according to Eq.4, secondly count normalized central moments  $I_1$  to  $I_6$ [16].

Table 1 offers dimensions of color, texture and shape features and shows the extraction of 39 dimension feature vector of image. Here number marks the dimensions of every feature.

Color(9)			Texture(22)		Shape(8)		
mean	MSE	entropy	LBP	GLCM	aspect ratio	roundness	Hu moment
3	3	3	18	4	1	1	6

TABLE I. DIMENSIONS OF THE FEATURES

#### IV. MEDICINE CLASSIFICATION BASED ON BP NEURAL NETWORK

The task that follows is to design classifier to correctly classify the feature vector. Forward feedback neural network is chose. Lippman holds only triple layer forward network is required to constitute arbitrary complex discriminant function.

##### A. BP network structure

Figure 5 shows the typical three-layer network, that is input-hidden layer- output. BP network structure with only one hidden layer is demonstrated in Fig. 5. Suppose

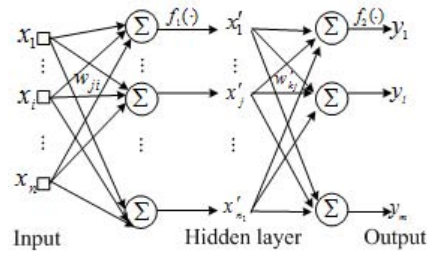


Figure 5. The sketch map of BP network structure with three-layer neurons

the input vector of BP network is  $x \in \mathbb{R}^n$ , i.e.  $x = (x_1, x_2, \dots, x_n)^T$ ;  $n_1$  neurons exist in the hidden layer and their output is  $x' \in \mathbb{R}^{n_1}, x' = (x'_1, x'_2, \dots, x'_{n_1})^T$ ;  $m$  neurons are in the output layer and their output is  $y \in \mathbb{R}^m$ , i.e.  $y = (y_1, y_2, \dots, y_m)^T$ . Imagine the weight from input layer to hidden layer is  $w_{ji}$ , the threshold is  $\theta_j$ . Suppose the weight from the hidden layer to output layer  $w'_{kj}$ , the threshold is  $\theta'_k$ . Thus the neuron output of every layer is

$$\begin{cases} x'_j = f_1(\sum_{i=1}^n w_{kj} x_i - \theta_j), & j = 1, 2, \dots, n_1 \\ y_k = f_2(\sum_{j=1}^{n_1} w'_{kj} x'_j - \theta'_k), & k = 1, 2, \dots, m \end{cases} \quad (14)$$

where  $f_1(\cdot)$  and  $f_2(\cdot)$  is called transition functions of each layer.

##### B. Chinese herbal medicine classification based on BP neural network

Feature vector made up of color, texture and shape features serves as input of neural network. Classification identifier serves as net output. Suppose the desired output

of the net  $d = 1, 2, \dots, M$ .  $M$  denotes the number of medicine classified.

(1) Define the network structure, namely determine the number of input, hidden and output layer neurons and set the maximum learning iterations, control precision and learning rate. Let transfer functions of each layer be

$$f_1(x) = \frac{1}{1 + e^{-x}}, f_2(x) = x$$

(2) Input  $x_i$  and desired output  $d_j$  are normalized to  $[-1, 1]$ .

$$x_i = -1 + \frac{2(x_i - x_{min})}{x_{max} - m_{min}} \quad (15)$$

$$d_j = -1 + \frac{2(d_j - 1)}{M - 1}$$

(3) Back error propagation algorithm[17] is adopted to train the network, and the network weights and thresholds are obtained.

(4) Concerning images to be identified, feature vectors of medicine are extracted according to Section 3. Then the normalization is carried out on the basis of Eq.15.

(5) Output of neural network  $y$  is worked out on the basis of Eq.14. Then inverse transformation is implemented by Eq.16, and map output  $y$  to interval  $[1, M]$ .

$$y = \left[ \frac{(y + 1)(M - 1)}{2} + 1.5 \right]$$

where  $[.]$  is Gauss integer function.

The final output is the index of classification label sets.

### V. EXPERIMENTAL RESULTS AND ANALYSIS

We analyzed 204 images of 8 kinds of Chinese herb medicine, namely areca catechu, nux vomica, pinellia ternate, gastrodia elata, radix curcumae, liriopie, ligusticum and hawthorn. Algorithm was implemented using Visual C++ 6.0 and Matlab 2010b development platform with Open CV 1.0 library. Abridged general view of Chinese herb medicine classification based on BPN is shown in Fig. 6. The white region in (b) is target region, namely ROI. The component of the color, texture and shape feature vector of the ROI is shown in (c) to (e). The outline and the minimum bounding rectangle is shown in Fig.7. The curve is the outline and the rectangle is the smallest bounding rectangle of ROI. The radar chart of 39-dimensional feature of the eight kinds of medicine is demonstrated in Fig.8. The data in the figure shows that these eight kinds of medicine differ greatly in mean value of color features, the second angular moment of texture features, contrast, relativity, the width-height ratio and roundness of shape feature. They can be differentiated on the basis of these features.

The input layer has thirty-nine neurons which coincide with the dimensions of feature vectors in neural network. The output layer has one neuron which the value corresponds to class label. Unfortunately the number of hidden layer neurons is indeterminable quantificationally. We randomly choose a half of all medicinal images as training samples. And the rest is test samples. Determine

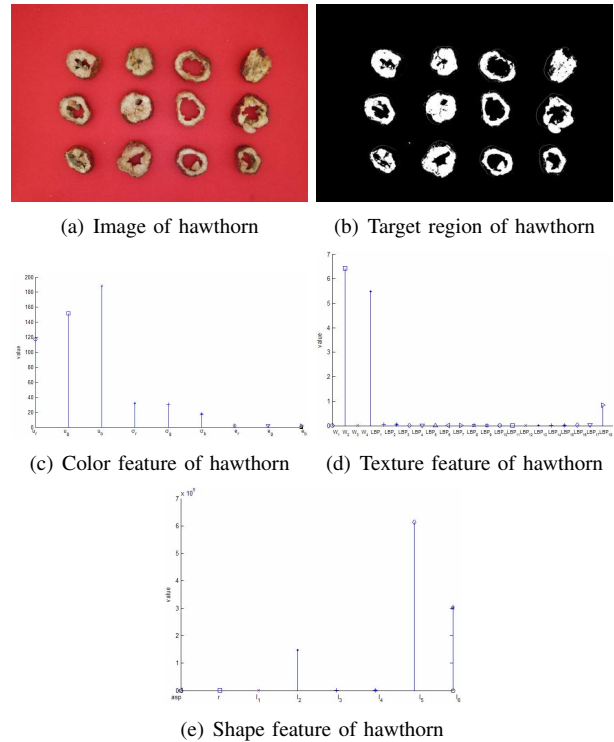


Figure 6. Chinese herbal medicine classification

the number of hidden layer neurons according to identification precision of test samples. The relationship between the number of hidden layer neurons and identification precision is shown in Fig.9. Select twelve hidden layer neurons in terms of efficiency and precision.

### VI. CONCLUSIONS

The herbal medicine classification based on BP neural network proposed in this paper could effectively classify the herbal medicine and be a computer assistant of medicine inspection. Color, texture and shape features are selected as medicinal features. The proposed approach could differentiate a majority of medicine. As for some medicine of special application such as sulfur smoked herbs, multi-sensor information fusion classification including image sensors, gas sensors and taste sensors could improve the inspection accuracy and expand the application.

### REFERENCES

- [1] Fong, Sophia YK, "Establishing the Pharmaceutical Quality of Chinese Herbal Medicine: A Provisional BCS Classification..," in *Molecular pharmaceutics*, 2013, pp. 1623-1643.
- [2] Hou, Xiaofang, "A vascular smooth muscle/cell membrane chromatography/Offline-gas chromatography/mass spectrometry method for recognition, separation and identification of active components from traditional Chinese medicines," in *ournal of Chromatography A*, 2009, pp. 7081-7087.
- [3] Fang, Xingchun, "Application of pyrolysis-high-resolution gas chromatography-pattern recognition to the identification of the Chinese traditional medicine mai dong," in *Journal of Chromatography A*, 1990, pp. 287-292.

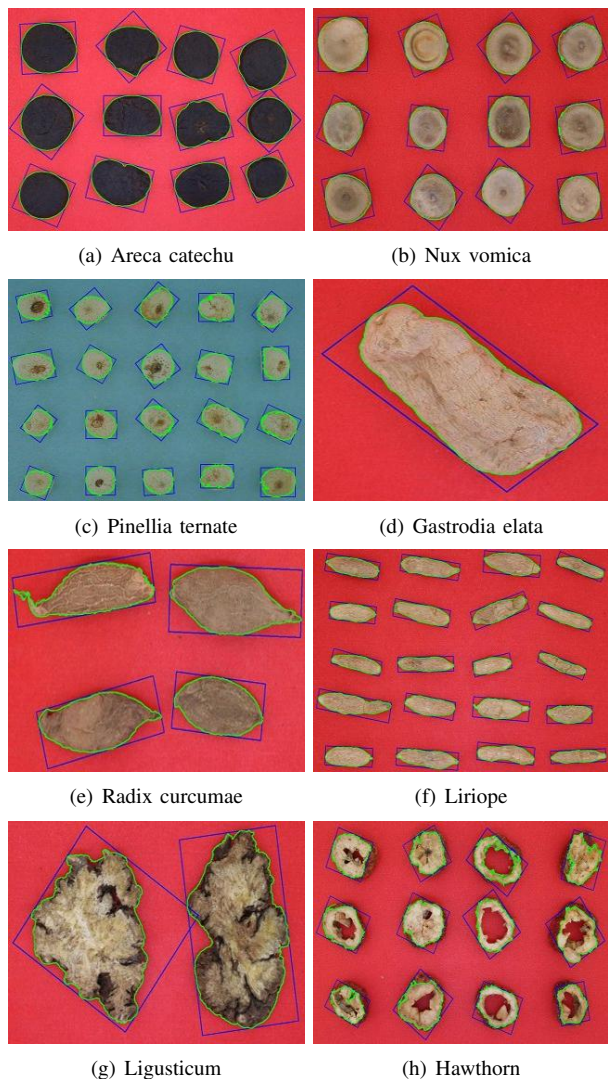


Figure 7. Outlines and bounding rectangles of Chinese herbal medicine

[4] Su, Xingye, "Affinity chromatography with immobilized DNA stationary phase for biological fingerprinting analysis of traditional Chinese medicines," *Journal of Chromatography A*, 2007, pp. 132–137.

[5] Xu, Chang-Hua, Multi-steps Infrared Macro-fingerprint Analysis for thermal processing of *< i > Fructus viticis*," *Vibrational spectroscopy*, 2006, pp. 118–125.

[6] Wu, Yan-Wen,, "Fourier transform mid-infrared (MIR) and near-infrared (NIR) spectroscopy for rapid quality assessment of Chinese medicine preparation Honghua Oil," *Journal of Pharmaceutical and Biomedical Analysis*, 2008, pp.498–504.

[7] Jiang Y, David B, Tu P, "Recent analytical approaches in quality control of traditional Chinese medicines—a review," *Analytica chimica acta*, 2010, pp.9–18.

[8] Zeng Z D, Chau F T, Chan H Y, "Recent advances in the compound-oriented and pattern-oriented approaches to the quality control of herbal medicines," *Chin Med*, 2008.

[9] Wang J, Kong H, Yuan Z, "A Novel Strategy to Evaluate the Quality of Traditional Chinese Medicine based on the Correlation Analysis of Chemical Fingerprint and Biological Effect," *Journal of pharmaceutical and biomedical analysis*, 2013, pp.57–64.

[10] Wang X, Zhang B, Guo Z, "Facial image medical analysis system using quantitative chromatic feature," *Expert*

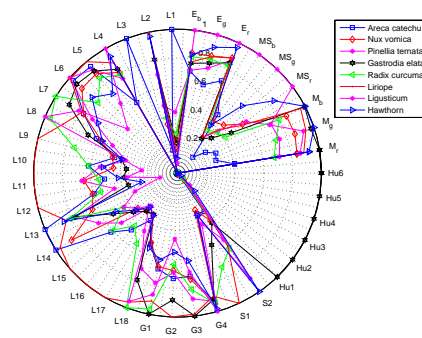


Figure 8. Feature visualization of the medicinal material based on radar diagram

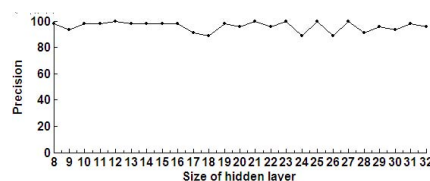


Figure 9. Relation between sizes of hidden layer and identification precision

*Systems with Applications*, 2013, pp.3738–3746.

[11] N. Otsu, "A Threshold Selection Method from Gray-Level Histograms," *IEEE Transactions on Systems*, 1979, pp.62–66.

[12] Ahonen T, Hadid A, Pietikainen M, "Face Recognition with Local Binary Patterns," *IEEE Transactions on Systems*, 2004, pp.469–481.

[13] Rodriguez Y, Marcel S, "Face authentication using adapted local binary Pattern histograms," *ECCV*, 2006, pp.321–332.

[14] Ojala T, Pietikainen M., Harwood D, "A comparative study of texture measures with Classification based on feature distributions," *Pattern Recognition*, 1996, pp.51–59.

[15] Haralick Robert M, Shanmugam K, "Texture features for image classification," *IEEE Transactions on Systems, Man and Cybernetics*, 1973, pp.610–621.

[16] MK Hu, "Visual Pattern Recognition by Moment Invariants," *IRE Transaction on Information Theory*, 1962, pp.179–187.

[17] Rumelhart D E, Hinton G E and Williams R J, "Learning representations by back-propagation errors," *Nature*, 1986, pp.533–536.

**Changjiang Liu** received B.S. from Chongqing Technology and Business University and M.S degree from Chongqing University in 2002 and 2008 respectively. He is now pursuing Ph.D. degree in the College of Computer Science, Sichuan University. Meanwhile, he is also working as an association professor in Sichuan University of Science & Engineering (SUSE). His research focused on image processing.

**Xuling Wu** received B.S. from China West Normal University and M.S degree from University of Electronic Science and Technology of China in 2004 and 2012 respectively. She is now working as a lecturer in SUSE. Her research focused on Foreign Linguistics and Applied Linguistics.

**Wei Xiong** is now pursuing Ph.D. degree in Sichuan University (SCU). Meanwhile, he is also working as a lecturer in SCU.